

ReCLIP: Refine Contrastive Language Image Pre-Training with Source Free Domain Adaptation

Xuefeng Hu¹ Ke Zhang² Lu Xia² Albert Chen² Jiajia Luo² Yuyin Sun²
Ken Wang² Nan Qiao² Xiao Zeng² Min Sun² Cheng-Hao Kuo² Ram Nevatia¹

¹University of Southern California ²Amazon

¹{xuefengh, nevatia}@usc.edu

²{kezha, luxial, aycchen, lujiajia, yuyinsun, zixiaow, qiaonan, zenxiao, minnsun, chkuo}@amazon.com

Abstract

Large-scale Pre-Training Vision-Language Model such as CLIP [32] has demonstrated outstanding performance in zero-shot classification, e.g. achieving 76.3% top-1 accuracy on ImageNet without seeing any example, which leads to potential benefits to many tasks that have no labeled data. However, while applying CLIP to a downstream target domain, the presence of visual and text domain gaps and cross-modality misalignment can greatly impact the model performance. To address such challenges, we propose ReCLIP, the first source-free domain adaptation method for vision-language models, which does not require any source data or target labeled data. ReCLIP first learns a projection space to mitigate the misaligned visual-text embeddings and learns pseudo labels, and then deploys cross-modality self-training with the pseudo labels, to update visual and text encoders, refine labels and reduce domain gaps and misalignments iteratively. With extensive experiments, we demonstrate ReCLIP reduces the average error rate of CLIP from 30.17% to 25.06% on 22 image classification benchmarks.

1. Introduction

Large-scale pre-training vision-language models such as CLIP [32] have emerged recently and formed a new paradigm in the task of image classification. Instead of matching images with category abstraction (label index), vision-language models match images towards text embeddings from their category names. With the help of semantic relationship from text embedding space, and large-scale pre-training over more than 400 millions of image-caption pairs, CLIP is capable of performing accurate image classification on novel target domains requiring zero training examples but only category names.

However, we still observe domain gaps from both image and text inputs that impact CLIP performance. Existence

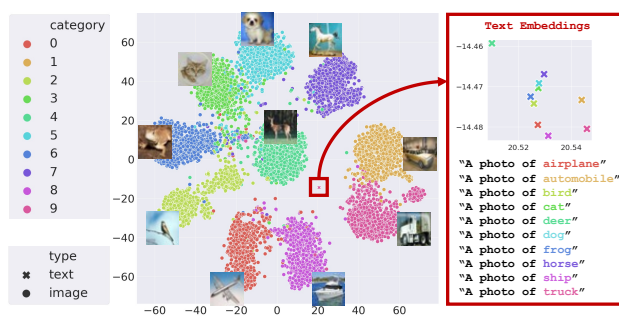


Figure 1. the t-SNE plot of visual and text embeddings from CLIP on CIFAR10 [23] test set. It is clear to see the misalignment in the vision-language space: the text embedding of a class name is adjacent to ones of other classes, but quite distant from image embeddings in the same class. Please refer to the text for further analysis and troubleshooting.

of visual domain gap between source and target images has been challenging for computer vision models [8, 42]. CLIP has been observed to have limitations on visual embedding when data comes from less common domains, e.g. Patch-Camelyon [40], CLEVR [19], etc. On the other hand, the domain gap on text is also a challenge for vision-language models. The performance of CLIP is often limited by the text embeddings rather than the visual embeddings, especially on fine-grained datasets e.g. RESISC45 [5], Birdsnap [2], where CLIP is able to create distinctive visual embeddings but the text embeddings from class names fail to capture discriminative information.

In addition to the gaps in the visual and text domains, we have identified significant misalignments between visual and text embeddings across most datasets. Figure 1 provides examples of this issue on the widely used benchmark CIFAR10. We believe that there are two primary reasons for these misalignments. Firstly, text embeddings may be redundant, as CLIP was trained to work with millions of captions and concepts, whereas target domain categories might only activate limited feature dimensions, leaving the

remaining ones inactive and redundant; these redundant dimensions can dominate the similarity calculation. Secondly, visual embeddings may contain a significant amount of class-agnostic information; since CLIP uses real captions for training, it preserves rich information, such as lighting, color, texture, and relationship but only a small portion of this information is crucial for classification.

Therefore, adaptation of both visual and text representations is crucial in improving the target domain performance of vision-language models like CLIP. However, traditional domain adaptation methods have significant limitations in this context. One major challenge is that these methods usually either require target domain labeled examples (e.g. semi-supervised domain adaptation [9, 33, 46]), or source domain examples (e.g., unsupervised domain adaptation [20, 29, 34]). However, in typical use cases of CLIP, user usually has access only to unlabeled target images, which requires source-free unsupervised domain adaptation that does not need source data or labeled target data. Another challenge is that existing methods assume conditions that may not hold for vision-language models. For instance, most existing methods [26, 41] assume a lightweight classifier, while a vision-language model uses a considerably larger text encoder to generate adaptive classification weights based on category descriptions. This additional module adds both flexibility and complexity to the adaptation process. Thus, the lack of labeled data from source and target domains and the presence of multiple adaptable modules have made it necessary to develop a novel source-free adaptation algorithm for vision-language models.

To take advantages of the unified vision-language space, and address the challenges on the visual and text domain gaps and cross-modality misalignment, we propose ReCLIP, a novel source-free domain adaptation method to **Refine CLIP** models. Firstly, ReCLIP addresses the misalignment of visual and text embeddings from CLIP by learning a projection subspace that removes redundant dimensions and class-agnostic information, thereby realigning the embeddings. After generating aligned embeddings, ReCLIP employs label propagation to produce pseudo labels, which significantly enhances classification accuracy in the target domain. Secondly, ReCLIP leverages cross-modality self-training with high-confidence pseudo labels to iteratively refine embedding spaces and label assignments. To achieve this, ReCLIP employs two parallel components to update text and visual encoders. The first component fine-tunes the text encoder while freezing the visual to pull the text embedding of a label closer to the embeddings of images assigned the label. Meanwhile, the second component fine-tunes the visual encoder to learn an embedding space where images under the same label are adjacent to each other and the text embedding of the label. During fine-tuning, each component learns cross-modality consistency

in the target domain, leading to new label assignments. ReCLIP selects labels agreed upon by both components as high-confidence ones for the next iteration. This iterative process improves the quality of visual and text embeddings and significantly enhances the assignment of pseudo labels.

Our contributions are summarized in the following:

- As the first work that studies the source-free adaptation problem of vision-language model, we enhanced the CLIP’s classification ability towards novel target domains without any labeled data;
- We identified the cross-modality mis-alignment issue between CLIP’s visual and language embeddings, and we proposed a novel projection-based method to address the issue;
- We proposed a novel cross-modality self-training algorithm with high quality commonly agreed pseudo labels leveraging cross-modality consistency to mitigate domain gaps from both visual and text inputs;
- With extensive experiments and ablation studies, we arrive at ReCLIP which produces consistent and significant improvements over CLIP and other baseline methods; ReCLIP improves the average accuracy of CLIP from 69.83% to 74.94% on 22 datasets.

2. Related Works

2.1. Large-Scale Vision-Language Models

Many large-scale pre-training vision-language models have been recently proposed and demonstrate impressive zero-shot classification ability, such as CLIP [32], ALIGN [17] that perform large-scale contrastive training for strong generalization ability, and DeCLIP [8], SLIP [28] that focus on efficient training with additional self-supervised objectives. Among all, CLIP is still one of the strongest model in zero-shot classification task that has publicly available model. Therefore, we use CLIP as our main baseline in this work.

CLIP performs simple contrastive learning over 400M pairs of images and captions by pushing the visual and text representation near if they are from the same pair and away if they are not. At inference stage, CLIP makes classification prediction by matching the visual embeddings of query images with the text embeddings of categories names (wrapped in template text such as “a photo of {}”), and selects the one category with highest cosine similarity as prediction. CLIP is capable of performing classification over novel tasks without any training example, as long as the category names are provided. CLIP has demonstrated outstanding zero-shot classification accuracy [32].

Limitation of CLIP CLIP achieves great zero-shot performance on many datasets. However, we still observe few conditions where CLIP’s performance might be improved.

1) Inaccurate Text Description According to CLIP [32], the accuracy of CLIP can be drastically improved when the classification weights are fully-supervised fine-tuned on certain datasets (e.g., On EuroSAT, accuracy of CLIP improved from 59.9% to 98.2% after fine-tuning the classification weights). This indicates that CLIP has good potential with its default visual representations, but the performance is limited by the quality of text-generated classification weights. This behavior is observed often on fine-grained datasets (e.g., AID [44], Birdsnap [2], FGVC [27], DTD [6], EuroSAT [15], *etc.*), where the class names might not fully capture the visual differences between classes (e.g., “737-200” and “747-200” are two classes from FGVC); **2) Visual Gap.** On some datasets, there are clear gaps for CLIP to be further improved even after the fully supervised fine-tuning on classification weight. For example, fine-tuned CLIP achieves only 42.9% on Country211 [32], and 85.97% on PatchCamelyon [40] (a binary classification task with state-of-the-art system achieves 97.50%). This indicates that the visual encoder of CLIP can also be further improved.

2.2. Unsupervised Domain Adaptation

Unsupervised Domain Adaptation (UDA) is a task aimed at improving target domain performance of models that were pre-trained on a related but different source domain. Many techniques have been developed [20, 29, 34, 37, 43]. However, most of those techniques are not ideal for the purpose of improving CLIP’s zero-shot performance, as they often require access to source domain training data, while we do not require to access CLIP’s training data. **Source-Free Adaptation** defines a more challenging setting than UDA, where training examples from both source and target domain are not available. Test-time Adaptation methods such as TTT [38] and TENT [41] performs source-free adaptation and can be directly applied during test-time. However, both of these methods adapt the model by changing the batch-normalization weights, while CLIP uses layer-normalization and their assumptions can not hold. SHOT [26] might be the most promising existing method among all, which does not require access to training examples from neither source nor target domain, and has less requirement of the model architecture. During unsupervised adaptation, SHOT updates the feature extractor with cluster-based pseudo labels and information entropy loss, while maintaining the classifier frozen. This simple but effective approach achieves the state-of-the-art performance on the task of source-free adaptation. As a method designed for a classic image classification pipeline, the choice of keeping the classifier frozen can provide stable and effective guidance during the adaptation. However, for vision-language models like CLIP this assumption might not hold, as the classification weights generated from category names may also experience domain gaps and need to be adapted.

3. Method

We describe our method **ReCLIP**, which **Refines CLIP’s** classification performance by accessing only to the pre-trained model and the following target domain data:

- Pre-trained vision-language model $M = \{M_T, M_V\}$, with text encoder M_T and visual encoder M_V ,
- Unlabeled target images $X = \{x_1, x_2, \dots, x_n\}$,
- Target class names $C = \{c_1, c_2, \dots, c_m\}$.

Our goal is to increase the classification accuracy of M on target data X . As the first method that studies the source-free adaptation problem for vision-language model, we approach this problem in two steps: (1) How to align visual and text embeddings by removing class-agnostic and redundant information in a learned projection space (Section 3.1). Then we show how to assign pseudo labels for images in the projection space via label propagation (Section 3.2); (2) How to utilize the pseudo labels to further mitigate the visual and text domain gaps by efficiently updating both visual and text encoders, we propose a cross-modality self-training algorithm which updates embeddings and pseudo labels in a iterative fashion (Section 3.3).

3.1. Projection Space to Align Visual and Text

Figure 1 demonstrates the misalignment issue of text and visual embeddings from CIFAR10 [23], which we have also observed over all the ablation datasets. The plot indicates that the text embeddings of different class names are closer to each other than to images in the corresponding categories. We also validate the misalignment with quantitative statistics, as shown in Figure 2. The average cosine similarity between text embeddings is 82% while the average similarity between visual and text embeddings from the same category is only 23%. This indicates that the unified vision-language space of CLIP is far from well aligned.

As highlighted in Section 1, although the visual and text embeddings from CLIP convey rich information, much of them could be redundant and class-agnostic to target classification tasks. This redundancy can result in misalignment between the text and visual embeddings. We hence propose a projection-based method to eliminate the redundancy from both visual and text embeddings.

Remove class-agnostic information from visual embeddings. A straightforward way to remove the class-agnostic information from visual features is just to project all the visual embeddings onto the span of text embeddings. Assuming we have a d dimensional representation space \mathcal{R}^d , and we have m classes whose text embeddings are $T = [t_1, \dots, t_m] \in \mathcal{R}^{m \times d}$, where $t_i = M_t(c_i)$ for $i \in \{1, 2, \dots, m\}$. With Singular Value Decomposition

$$U, S, V = \text{svd}(T)$$

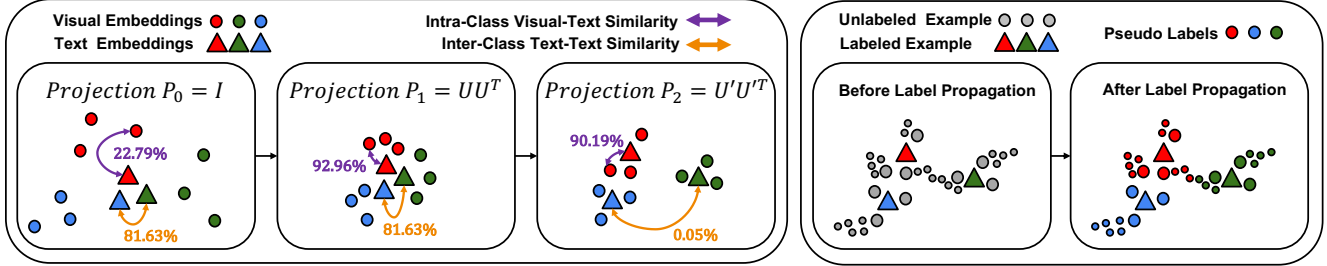


Figure 2. Demonstration on Feature Redundancy Removal (left) and Label Propagation (right). **Left:** P_0 shows the original distribution of visual and text embeddings of CLIP, where text embeddings are close to each other distant from visual embeddings; $P_1 = UU^\top$ removes the class agnostic information from visual embeddings, and has pulled closer visual and text embeddings. $P_2 = U'U'^\top$ separates the text embeddings away by removing the redundant information from them. Similarity values demonstrated in this example is calculated based on average statistics from CIFAR10 test set; **Right:** the Label Propagation process generates pseudo labels for unlabeled training images by propagating label information from labeled text embeddings (categories names) to unlabeled visual embeddings (training images) through nearest-neighbor connections.

we get $U = [e_1, e_2, \dots, e_m]$ as the orthonormal basis of the span of T , which defines a projection matrix $P_1 = UU^\top$. Then, $\forall f \in \mathcal{R}^d$, we can calculate $f' = fP_1$ with

$$e_k \cdot (f - f') = 0, \forall k \in \{1, \dots, m\}$$

where $f - f'$ is the class-agnostic information that does not contribute to the classification. As shown in Figure 2, P_1 increases the average similarity between images and text embeddings from the same category to 92.96% on CIFAR10.

Remove redundant information from text embeddings. As suggested in Principal Component Analysis, the first dimension e_1 of the outer-space basis U will be the major component that most $\{t_1, \dots, t_m\}$ overlap on. Removing the major component e_1 will make all text embeddings nearly perpendicular to each other. Therefore, with $U' = [e_2, e_3, \dots, e_m]$ we define a new projection matrix $P_2 = U'U'^\top$. As shown in Figure 2, P_2 successfully separates the text embeddings from different classes to an average cosine similarity of 0.05%, while maintaining high intra-class visual-text similarity at 90.19% on CIFAR10.

In addition to the improvement of CIFAR10 statistics, experiments on pseudo label generation also indicate the effectiveness of embedding space induced by P_2 in improving clustering performance, as demonstrated in Section 5.2.2.

3.2. Pseudo Label Generation for Vision-Language Model

The projection matrix P_2 removes the redundancies and aligns visual and text embeddings, which enables the generation of pseudo labels through Label Propagation [16], which is a semi-supervised learning method that propagates label information from labeled to unlabeled data points through nearest neighbor connections, as demonstrated in Figure 2. Although in source-free adaptation we do not have access to labeled data points, the embedding alignment through P_2 has enabled us to treat text embeddings

from class names as labeled points, and visual embeddings from images as unlabeled points.

With labeled examples $\{\hat{t}_i\}_{i=1}^m$ (class name embeddings) and unlabeled examples $\{\hat{v}_j\}_{j=1}^n$ (image visual embeddings), we make the union set L :

$$L = [\hat{t}_1, \hat{t}_2, \dots, \hat{t}_m, \hat{v}_1, \hat{v}_2, \dots, \hat{v}_n] \in \mathcal{R}^{d \times (m+n)}$$

Following Label Propagation [16], we first produce affinity matrix A_k through k -nearest neighbor affinity ranking $A_k = \text{top}^k(L^\top L)$ where $\text{top}^k(\cdot)$ is an operation that keeps the top k highest value per row from the full affinity matrix $L^\top L$. Then, with normalization and symmetrization, we have:

$$\mathcal{W} = D^{-\frac{1}{2}}(A_k + A_k^\top)D^{-\frac{1}{2}}$$

where $D := \text{diag}(W\mathbf{1}_{m+n})$ is the degree matrix, $\mathbf{1}_{m+n}$ is the all-ones $(m+n)$ -vector, and \mathcal{W} is the normalized adjacency matrix that defines the random walk probability. With an label matrix $Y \in \mathcal{R}^{(m+n) \times m}$ is defined with elements

$$Y_{ji} := \begin{cases} 1, & \text{if } j = i, j \leq m \\ 0, & \text{otherwise} \end{cases}$$

where Y_{ji} is 1 for the text embedding entries at the corresponding column, and 0 otherwise. Then, the pseudo label vector Z can be estimated by solving the random walk problem with initial state Y , propagation probability matrix \mathcal{W} and diffusion magnitude α :

$$Z := (\mathbf{I} - \alpha\mathcal{W})^{-1}Y \quad (1)$$

where $(\mathbf{I} - \alpha\mathcal{W})^{-1}$ is the closed-form solution to the random walk problem. As $(\mathbf{I} - \alpha\mathcal{W}) \in \mathcal{R}^{m+n}$ is not sparse, and therefore the calculation of its inverse matrix is very time consuming, we use conjugate gradient (CG) to approximately solve Equation 1, following the suggestion from

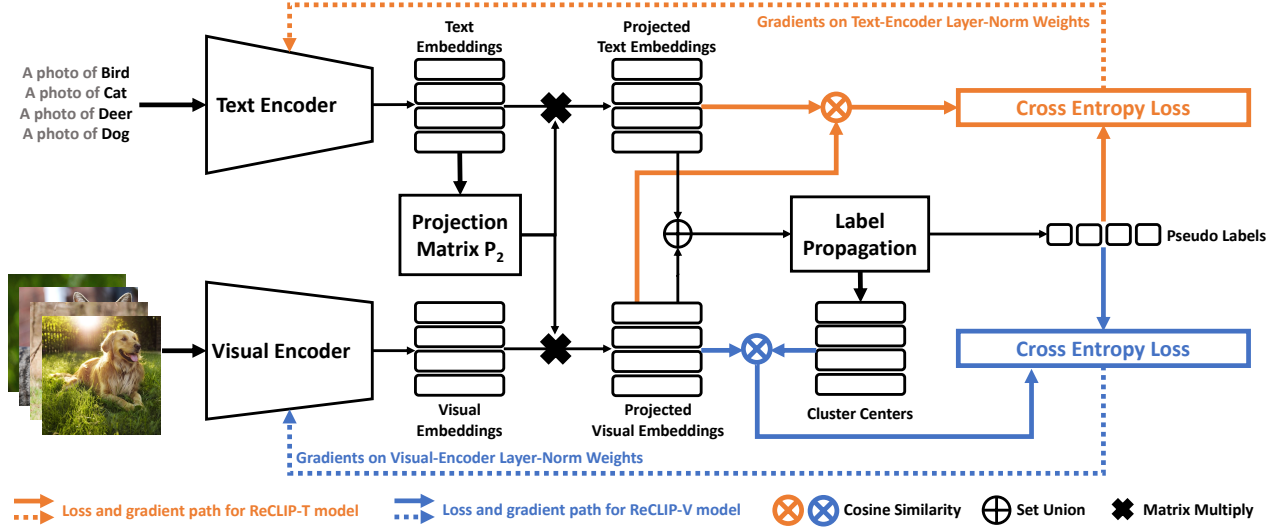


Figure 3. Flow Chart of ReCLIP-V and ReCLIP-T. Orange symbols describe the loss and gradients path of ReCLIP-V, and blue symbols describe the loss and gradients path of ReCLIP-T. Black symbols describe the common steps that both ReCLIP-V and ReCLIP-T have.

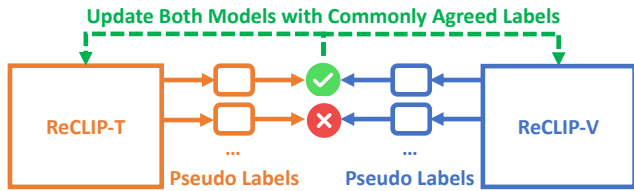


Figure 4. Flow Chart of Pseudo Labels Sharing. The cross-modality self-training algorithm merges the pseudo labels from ReCLIP-T and ReCLIP-V at the end of each epoch and updates the encoders only on high-confidence pseudo labels agreed by both.

[16]. Finally, with Equation 1 solved, the pseudo label can be given by

$$\tilde{y}_j := \arg \max_i z_{m+j,i}$$

where \tilde{y}_j is the pseudo label of image x_j , and z_{ji} is the (j, i) element of matrix Z .

3.3. Source-Free Adaptation for Vision-Language Model via Cross-Modality Self-Training

Vision-language models present a new challenge to adaptation algorithm, where both visual and text encoders need to be adapted. In this section, we discuss how to mitigate the domain gaps of visual and text domains, and propose a cross-modality self-training algorithm with pseudo labels from 3.2 to iteratively update the label assignments, and the visual and text encoders.

The self-training algorithm of ReCLIP consists of two parallel components: ReCLIP-T aims at closing text domain gap by pushing text embeddings towards visual embeddings of same class, by fine-tuning the text encoder with

the visual encoder frozen. ReCLIP-V aims at closing the visual domain gap by pushing visual embeddings of same class closer to each other, by fine-tuning the visual encoder with the text encoder frozen. On top of ReCLIP-V and ReCLIP-T, we integrate the pseudo labels by filtering the commonly-agreed ones to produce high-confidence training signals. For inference, we add the prediction logits from both ReCLIP-V and ReCLIP-T to make final prediction.

ReCLIP-T: Text Encoder Training. We optimize the text encoder M_t with simple cross-entropy loss $Loss^T := CE(\hat{Y}^T, \tilde{Y})$ between pseudo label \tilde{Y} and cosine similarity prediction logits $\hat{Y}^T = [\hat{v}_1, \dots, \hat{v}_n]^\top [\hat{t}_1, \dots, \hat{t}_m]$. The objective of adaptation on the text encoder is to push text embeddings $\{\hat{t}_i\}$ closer to the image embeddings $\{\hat{v}_j\}$ from the same class based on pseudo label assignments \tilde{Y}^T . In Figure 3 we present the details of ReCLIP-T, the detailed algorithm is provided in the supplementary materials.

ReCLIP-V: Visual Encoder Training. The goal of visual encoder adaptation is to push visual embeddings $\{\hat{v}_j\}$ from the same class to be closer to each other, to form a better feature space for classification. As contrastive loss is expensive and applying constraints on batch size, we have instead chosen to push visual embeddings closer to the center of its class instead of other visual embeddings as an alternative resort. To be specific, in ReCLIP-V we optimize the visual encoder M_v with cross-entropy loss $Loss^V := CE(\hat{Y}^V, \tilde{Y})$ between pseudo label \tilde{Y} and cosine similarity logits $\hat{Y}^V = [\hat{v}_1, \dots, \hat{v}_n]^\top [\hat{w}_1, \dots, \hat{w}_m]$, where $\hat{w}_1, \dots, \hat{w}_m$ are the class centers calculated based on \tilde{Y} . In Figure 3 we present the details of ReCLIP-V, the detailed algorithm is provided in the supplementary materials.

High-Confidence Pseudo Labels Sharing. ReCLIP-V

updates the similarities among visual embeddings with $Loss^V$, while ReCLIP-T updates the projection matrix and text embeddings with $Loss^T$. As these two modules separately optimize the visual and text encoders with different objectives, their pseudo labels may start to diverge after a certain number of epochs, resulting in different views where only the commonly agreed samples are likely to be correctly classified. As such, ReCLIP collects pseudo labels from both ReCLIP-V and ReCLIP-T at the end of each epoch, and updates both models with only the commonly agreed pseudo labels \tilde{Y} , as illustrated in Figure 4. The detailed algorithm is provided in supplementary materials.

4. Experiment

4.1. Datasets and Evaluation

Radford *et al.* [32] reported CLIP performances on 27 standard benchmarks. We evaluate our model on 21 of these benchmarks except: 1) KITTI [14], UCF101 [35], VOC2007 [13], Kinetics700 [4] that are object detection or video classification benchmarks that are out of the scope of our discussion; 2) HatefulMemes [21] and CLEVR [19], where CLIP [32] are evaluated on custom splits that are not released at the time of this submission.

Additionally, we have extended the list to include one of our ablation dataset, AID [44]. We are reporting scores on 22 benchmarks in total. For all benchmarks, we use top-1 classification accuracy as our metric unless otherwise specified. During adaptation, ReCLIP performs self-training on the unlabeled test data of each dataset in a transductive manner. The inference is then similar to CLIP after adaptation.

4.2. Implementation Details

We used the ViT/L-14 checkpoints from CLIP as our base model for ReCLIP. We used AID, CIFAR10 and CIFAR100 as our ablation datasets where we perform ablation studies and find the best hyper parameters.

We keep most of the text/visual encoder parameters frozen and only update the layer-normalization [1] weights, as it is shown to be one of the most effective and stable option to adapt models with noisy supervision [41]. More discussion on learnable module choices is covered in Table 5.

For the self-training of ReCLIP, we use SGD as optimizer with learning rate of 10^{-3} , weight decay of 10^{-4} and momentum of 0.9 on both visual and text encoders, with maximum length set to be $\min\{5000 \text{ iterations}, 50 \text{ epochs}\}$. Datasets with more classes require more memory to generate text embeddings. Therefore, we use batch size of 32 for datasets with more than 200 categories (Birdsnap, Country211, SUN397, ImageNet), and batch size of 64 for the other datasets. For Label Propagation, we use propagation strength $\alpha = 0.99$ and neighbor size $k = 20$. We use the same set of hyper parameters on all ReCLIP experiments

unless otherwise specified.

For datasets with more than 500 classes (Birdsnap, ImageNet), we notice the accuracy of pseudo labels generated by label propagation becomes unstable, and it requires additional hyper-parameter tuning to achieve good performance. To maintain stable performance, we turn off label propagation and simply use model predictions as pseudo labels on datasets with over 500 categories (Birdsnap, ImageNet). For all other datasets, we follow the exact process as described in Section 3.3.

For SHOT, we merged CLIP into its pipeline. We used its default SGD optimizer with learning rate of 10^{-6} , weight decay of 10^{-4} and momentum of 0.9, with batch size of 64 and maximum epoch 50.

5. Results

5.1. Main Result

In Table 1 we present the source-free adaptation accuracy of ReCLIP over 22 datasets. For comparison, we present the following methods:

- CLIP [32]: State-of-the-art zero-shot image classification model. We present both the accuracy reported in [32] (*report*) and the one from our replication for each dataset (*repro*).
- SHOT [26]: State-of-the-art source-free unsupervised adaptation method. We report the classification accuracy after adaptation on the target dataset.

Besides the accuracy from final epoch of self-training, we report the accuracy from the peak-performing epoch for SHOT and ReCLIP as well, denoted as *peak*.

As shown in Table 1, ReCLIP achieves consistent and significant improvements over CLIP on 21 datasets and comparable performance on Country 211. ReCLIP decreases CLIP’s average error rates from 30.17% to 25.06%, a 17% relative improvement. ReCLIP achieves further gains at peak performance, lowering average error rates to 24.15% and improving 20% relative to CLIP.

On simple datasets such as MNIST, STL10, CIFAR10, and CIFAR100 where SHOT was originally tested on [26], SHOT did not drop much performance on the final epoch compared to its peak. However, on many other datasets, we observe a significant performance drop at the final epochs. Comparing the peak and final epoch performance, SHOT lost 19.01% while ReCLIP only lost 0.91%. This indicates that our self-training algorithm is effective in stabilizing the noisy unsupervised adaptation process. On the other hand, even at peak epochs, SHOT gets significantly less improvement than ReCLIP. One possible reason is that SHOT only updates the visual feature extractor and keeps the classifier part frozen, which has limited its performance. As we mentioned in Section 2.1, the classification weights from CLIP

	Avg Acc	AID [44]	Birdsnap [2]	Caltech101 [24]	CIFAR10 [23]	CIFAR100 [23]	Country211 [32]	DTD [6]	EuroSAT [15]	FEER2013 [47]	FGVC [27]	Flowers [30]	Food101 [3]	GTSRB [36]	ImageNet [10]	MINIST [11]	Oxford Pet [31]	PCam [40]	SST2 [32]	RESISC45 [5]	Cars [22]	STL10 [7]	SUN397 [45]
CLIP <i>report</i>	70.08	-	48.30	92.6*	96.20	77.90	32.70	55.30	59.90	57.50	36.1*	78.7*	92.90	50.30	75.30	87.20	93.50	58.80	64.00	71.60	77.3*	99.30	67.70
CLIP <i>repro</i>	69.83	68.73	52.48	91.63	95.60	78.22	31.84	55.37	60.00	56.39	31.59	79.04	93.08	50.59	75.52	76.23	93.62	62.43	68.92	69.66	77.88	99.36	67.97
SHOT	36.48	42.93	0.27	5.05	95.84	79.47	0.55	55.32	24.03	18.03	1.65	1.43	1.00	32.84	0.10	84.14	93.51	67.61	49.92	2.05	0.6	99.28	46.9
SHOT <i>peak</i>	55.49	70.03	51.67	91.85	96.31	79.47	0.67	55.48	24.03	54.42	31.98	8.39	1.89	53.21	0.10	87.99	93.62	67.61	70.29	54.76	77.35	99.40	50.29
ReCLIP	74.94	77.97	52.96	93.02	96.95	82.32	31.92	60.85	78.75	58.07	36.63	82.05	94.15	66.81	75.81	90.88	95.61	70.15	73.48	78.41	77.96	99.58	74.41
ReCLIP <i>peak</i>	75.85	79.27	53.28	93.10	97.04	83.42	31.95	61.38	79.94	58.29	38.70	83.14	94.18	69.14	76.01	97.11	96.05	70.56	73.48	79.31	79.26	99.59	74.53

Table 1. Classification accuracies (%) on 22 benchmarks. * on FGVC, Caltech101, Oxford-IIIT Pet and Flowers102, CLIP reported mean-class-accuracy. All other scores in this table are top-1 accuracy.

	CIFAR10	CIFAR100	AID
Vanilla CLIP	95.54	76.48	64.87
Label Propagation	96.38	80.66	74.73
ReCLIP-V	96.69	80.84	79.47
ReCLIP-T	96.50	81.10	79.07
ReCLIP (w/o Label Sharing)	97.40	82.80	80.01
ReCLIP (w/ Label Sharing)	97.48	84.14	82.53

Table 2. Comparison of classification accuracy with different version ReCLIP on ablation datasets. ReCLIP with Label Sharing (Figure 4) is shown to be most effective compared to ReCLIP-V, ReCLIP-T (Figure 3) and their simply assembled predictions (ReCLIP w/o Label Sharing).

can also be improved, especially when the category names are not accurate. This comparison indicates the advantage of ReCLIP in adapting vision-language models.

As both SHOT and ReCLIP use pseudo labels to perform adaptation, we have also observed that the pseudo labels from ReCLIP are more stable than the ones by SHOT. Detailed comparison on pseudo label quality of SHOT and ReCLIP is provided in the supplementary materials.

For Country211, as we briefly mentioned in Section 2.1, Country211 is designed to predict geo-location based on visual appearance, while CLIP might tend to describe the image from actual content and texture. As shown in [32], CLIP can only achieve 42.9% after its classifier is fine-tuned in the fully supervised way. Therefore, it might be challenging to obtain improvement during unsupervised adaptation.

Runtime and Inductive Performance Despite the original CLIP pre-training took 73728 GPU-hours on V100 GPU [32]), self-training of ReCLIP is very efficient, which completes adaptation in only 0.5 to 5 GPU-Hour on V100, depends on the target dataset size. Note that this adaptation time is a one-time effort on each target domain and ReCLIP can then inference on unseen data from the same domain without re-training. Besides the transductive results provided in Table 1, we also run ReCLIP in a inductive setting, where ReCLIP performs self-training on the training split of a dataset (0.5 to 5 GPU-Hour), and inference on the test split

	AID	CIFAR10	CIFAR100
Vanilla CLIP	68.80	95.59	78.21
Hierarchical Clustering	55.20	36.52	9.27
Spectrum Clustering	68.10	61.25	57.35
k -means Clustering	72.73	95.07	49.43
k -NN Classifier (P_0)	72.30	93.74	69.46
k -NN Classifier (P_1)	72.76	95.77	77.81
k -NN Classifier (P_2)	72.43	95.76	78.19
Label Propagation (P_0)	60.80	94.01	63.58
Label Propagation (P_1)	60.43	96.23	45.41
Label Propagation (P_2)	76.36	96.31	81.56

Table 3. Pseudo label accuracy with different methods. Label Propagation on projection space P_2 is shown to be the most effective and stable method in generating accurate pseudo labels.

(similar to CLIP inference time). ReCLIP achieves similar improvements in the inductive setting: 96.92%, 82.30% and 79.87% accuracy on the test sets of CIFAR10, CIFAR100 and AID, respectively. More results in inductive setting is also available in Section 5.2.

5.2. Ablations Studies

In this section, we present the ablation studies on choices of learnable modules, pseudo label generation, and a comparison of different ReCLIP versions. We use AID, CIFAR10, and CIFAR100 as our ablation datasets, and the test set of each dataset is equally split into two fixed partitions. We report all ablation results in an inductive manner where models are first trained on partition 1 and then evaluated on partition 2. Note that results in this section is not directly comparable to 5.1 because the different evaluation partition.

5.2.1 Effectiveness of ReCLIP Components

In Table 2 we present the comparison between different versions of ReCLIP. As shown, Label Propagation can create pseudo labels with significantly improved accuracy compared to vanilla CLIP. On the top of Label Propagation, both

	CIFAR10		CIFAR100		AID	
	Original	→ ReCLIP	Original	→ ReCLIP	Original	→ ReCLIP
SLIP (ViT-L/16)	89.45	→ 91.80	56.69	→ 67.61	48.13	→ 64.07
DeCLIP (ViT-B/32)	90.57	→ 94.50	66.58	→ 77.10	53.53	→ 65.93
CLIP (RN50)	71.46	→ 82.73	42.32	→ 53.15	53.43	→ 65.97
CLIP (ViT-B/32)	89.83	→ 92.15	65.25	→ 71.09	60.83	→ 76.80

Table 4. Ablation Studies on the effectiveness of ReCLIP on different model architecture and pre-training strategies.

ReCLIP-V and ReCLIP-T (Figure 3) are shown to be effective in providing further improvements. In ReCLIP(w/o Label Sharing) we present the result by simply assembling predictions from separately trained ReCLIP-V and ReCLIP-T at inference time. Comparing the last two rows of Table 2 we observe that ReCLIP (w/ Label Sharing) has clear improvement over ReCLIP (w/o Label Sharing), which indicates that the commonly agreed pseudo-labels stabilizes the noisy adaptation process and improved both ReCLIP-V and ReCLIP-T to achieve better performance.

5.2.2 Comparison on Pseudo Label Generations

In Table 3, we compare methods in pseudo label generation. For clustering based methods, we assign the same pseudo labels for examples from the same cluster, based on the in-cluster majority vote; For k -NN Classifier and Label Propagation methods, we experiment them on original CLIP feature space P_0 , and on projection spaces P_1, P_2 as described in Figure 2. For k -NN Classifiers, we assign each example with the major vote prediction within its k -nearest-neighborhood, with k equal to the average sample count per class. For Label Propagation on P_0 , we select the example with the highest confidence from each class as the labeled example to perform label propagation as a baseline. Label Propagation on P_1, P_2 are as described in Section 3.1.

Table 3 indicates k -NN based methods achieve better performance on projection spaces P_1 are P_2 , which indicates the effectiveness of P_1, P_2 in refining CLIP’s visual embeddings. On Label Propagation methods, P_2 gives a significant improvement over P_0, P_1 , indicating its effectiveness in aligning CLIP’s visual and text embeddings.

5.2.3 Comparison on other Vision-Language Models

ReCLIP is designed to improve the classification performance of visual-language models in general, not only on CLIP. We tested the effectiveness of ReCLIP on SLIP [28] and DeCLIP [25], both of these improved CLIP by adding self-supervision learning objectives during pre-training. We have also tested ReCLIP on other versions of CLIP with smaller architectures. As shown in Table 4, ReCLIP demonstrates steady and significant improvements on various vision-language models and architectures.

	CIFAR10	CIFAR100	AID
Vanilla CLIP	95.54	76.48	64.87
Learnable Text Prompts	97.50	82.18	93.73
Learnable Visual Prompts [18]	96.70	80.68	74.27
Text Encoder Layer-Norm	97.32	83.30	94.8
Visual Encoder Layer-Norm	97.8	85.16	69.40

Table 5. Fully supervised fine-tuning accuracy of CLIP with different learnable modules on ablation datasets. On AID, fine-tuning weights from Text Encoder Layer-Norm is shown to be most effective; On CIFAR10 and CIFAR100, fine-tuning weights from Visual Encoder Layer-Norm is shown to be most effective.

5.2.4 Comparison of Learnable Modules

In Table 5, we evaluate different learnable modules by comparing their fully-supervised fine-tuned performance. As suggested in [41], fine-tuning the normalization weights is shown to be efficient and stable, compared to fine-tuning the entire weights in self-training of ReCLIP. Recent research [18] also suggests that learnable prompts can also be effective in providing stable and fast performance improvement during the fine-tuning of Transformer [12, 39] based models. In Table 5, we perform Visual Prompt tuning following [18], and our own designed Text Prompt. Due to the space capacity, details of the learnable text prompt will be covered in the supplementary material.

As shown in Table 5, fine-tuning Layer-Norm weights from Visual Encoder has the best fully supervised accuracy on both CIFAR10 and CIFAR100, while fine-tuning Layer-Norm weights from Text Encoder has the best fully supervised accuracy on AID. As described in Section 2.1, on some datasets (including AID), the performance CLIP is mainly limited by the poor quality text embeddings from inaccurate class names. In this case, fine-tuning the text encoder will achieve better performance as we observed. Table 5 results suggest the necessity of fine-tuning CLIP from both the visual and text side to handle different scenarios.

6. Conclusion

In this paper, we introduce ReCLIP, a novel solution on source-free domain adaptation for vision-language models. Our method aims to mitigate the gap between visual and text domains and address cross-modality misalignment. ReCLIP firstly removes redundant information from CLIP embeddings using a novel designed projection space and realigns visual and text embeddings to generate dependable pseudo labels for target classification tasks. ReCLIP further applies cross-modality self-training with pseudo labels, which iteratively enhances label assignments and visual and text embeddings. ReCLIP significantly improves CLIP, increasing the average accuracy from 69.83% to 74.94% across 22 datasets, as shown in extensive experiments.

References

- [1] Jimmy Lei Ba, Jamie Ryan Kiros, and Geoffrey E Hinton. Layer normalization. *arXiv preprint arXiv:1607.06450*, 2016. 6
- [2] Thomas Berg, Jiongxin Liu, Seung Woo Lee, Michelle L Alexander, David W Jacobs, and Peter N Belhumeur. Birdsnap: Large-scale fine-grained visual categorization of birds. In *Proceedings of the IEEE Conference on Computer Vision and Pattern Recognition*, pages 2011–2018, 2014. 1, 3, 7
- [3] Lukas Bossard, Matthieu Guillaumin, and Luc Van Gool. Food-101—mining discriminative components with random forests. In *European conference on computer vision*, pages 446–461. Springer, 2014. 7
- [4] Joao Carreira and Andrew Zisserman. Quo vadis, action recognition? a new model and the kinetics dataset. In *proceedings of the IEEE Conference on Computer Vision and Pattern Recognition*, pages 6299–6308, 2017. 6
- [5] Gong Cheng, Junwei Han, and Xiaoqiang Lu. Remote sensing image scene classification: Benchmark and state of the art. *Proceedings of the IEEE*, 105(10):1865–1883, 2017. 1, 7
- [6] M. Cimpoi, S. Maji, I. Kokkinos, S. Mohamed, , and A. Vedaldi. Describing textures in the wild. In *Proceedings of the IEEE Conf. on Computer Vision and Pattern Recognition (CVPR)*, 2014. 3, 7
- [7] Adam Coates, Andrew Ng, and Honglak Lee. An analysis of single-layer networks in unsupervised feature learning. In *Proceedings of the fourteenth international conference on artificial intelligence and statistics*, pages 215–223. JMLR Workshop and Conference Proceedings, 2011. 7
- [8] Gabriela Csurka. Domain adaptation for visual applications: A comprehensive survey. *arXiv preprint arXiv:1702.05374*, 2017. 1, 2
- [9] Hal Daumé III, Abhishek Kumar, and Avishek Saha. Frustratingly easy semi-supervised domain adaptation. In *Proceedings of the 2010 Workshop on Domain Adaptation for Natural Language Processing*, pages 53–59, 2010. 2
- [10] Jia Deng, Wei Dong, Richard Socher, Li-Jia Li, Kai Li, and Li Fei-Fei. Imagenet: A large-scale hierarchical image database. In *2009 IEEE conference on computer vision and pattern recognition*, pages 248–255. Ieee, 2009. 7
- [11] Li Deng. The mnist database of handwritten digit images for machine learning research. *IEEE Signal Processing Magazine*, 29(6):141–142, 2012. 7
- [12] Alexey Dosovitskiy, Lucas Beyer, Alexander Kolesnikov, Dirk Weissenborn, Xiaohua Zhai, Thomas Unterthiner, Mostafa Dehghani, Matthias Minderer, Georg Heigold, Sylvain Gelly, et al. An image is worth 16x16 words: Transformers for image recognition at scale. *arXiv preprint arXiv:2010.11929*, 2020. 8
- [13] M. Everingham, L. Van Gool, C. K. I. Williams, J. Winn, and A. Zisserman. The PASCAL Visual Object Classes Challenge 2007 (VOC2007) Results. <http://www.pascal-network.org/challenges/VOC/voc2007/workshop/index.html>. 6
- [14] Andreas Geiger, Philip Lenz, Christoph Stiller, and Raquel Urtasun. Vision meets robotics: The kitti dataset. *The International Journal of Robotics Research*, 32(11):1231–1237, 2013. 6
- [15] Patrick Helber, Benjamin Bischke, Andreas Dengel, and Damian Borth. Eurosat: A novel dataset and deep learning benchmark for land use and land cover classification. *IEEE Journal of Selected Topics in Applied Earth Observations and Remote Sensing*, 12(7):2217–2226, 2019. 3, 7
- [16] Ahmet Iscen, Giorgos Tolias, Yannis Avrithis, and Ondrej Chum. Label propagation for deep semi-supervised learning. In *Proceedings of the IEEE/CVF Conference on Computer Vision and Pattern Recognition*, pages 5070–5079, 2019. 4, 5
- [17] Chao Jia, Yinfei Yang, Ye Xia, Yi-Ting Chen, Zarana Parekh, Hieu Pham, Quoc Le, Yun-Hsuan Sung, Zhen Li, and Tom Duerig. Scaling up visual and vision-language representation learning with noisy text supervision. In *International Conference on Machine Learning*, pages 4904–4916. PMLR, 2021. 2
- [18] Menglin Jia, Luming Tang, Bor-Chun Chen, Claire Cardie, Serge Belongie, Bharath Hariharan, and Ser-Nam Lim. Visual prompt tuning. *arXiv preprint arXiv:2203.12119*, 2022. 8
- [19] Justin Johnson, Bharath Hariharan, Laurens Van Der Maaten, Li Fei-Fei, C Lawrence Zitnick, and Ross Girshick. Clevr: A diagnostic dataset for compositional language and elementary visual reasoning. In *Proceedings of the IEEE conference on computer vision and pattern recognition*, pages 2901–2910, 2017. 1, 6
- [20] Guoliang Kang, Lu Jiang, Yi Yang, and Alexander G Hauptmann. Contrastive adaptation network for unsupervised domain adaptation. In *Proceedings of the IEEE/CVF Conference on Computer Vision and Pattern Recognition*, pages 4893–4902, 2019. 2, 3
- [21] Douwe Kiela, Hamed Firooz, Aravind Mohan, Vedanuj Goswami, Amanpreet Singh, Pratik Ringshia, and Davide Testuggine. The hateful memes challenge: Detecting hate speech in multimodal memes. *Advances in Neural Information Processing Systems*, 33:2611–2624, 2020. 6
- [22] Jonathan Krause, Michael Stark, Jia Deng, and Li Fei-Fei. 3d object representations for fine-grained categorization. In *4th International IEEE Workshop on 3D Representation and Recognition (3dRR-13)*, Sydney, Australia, 2013. 7
- [23] Alex Krizhevsky, Geoffrey Hinton, et al. Learning multiple layers of features from tiny images. 2009. 1, 3, 7
- [24] Li, Andreeto, Ranzato, and Perona. Caltech 101, Apr 2022. 7
- [25] Yangguang Li, Feng Liang, Lichen Zhao, Yufeng Cui, Wanli Ouyang, Jing Shao, Fengwei Yu, and Junjie Yan. Supervision exists everywhere: A data efficient contrastive language-image pre-training paradigm. *arXiv preprint arXiv:2110.05208*, 2021. 8
- [26] Jian Liang, Dapeng Hu, and Jiashi Feng. Do we really need to access the source data? source hypothesis transfer for unsupervised domain adaptation. In *International Conference on Machine Learning*, pages 6028–6039. PMLR, 2020. 2, 3, 6

- [27] S. Maji, J. Kannala, E. Rahtu, M. Blaschko, and A. Vedaldi. Fine-grained visual classification of aircraft. Technical report, 2013. [3](#), [7](#)
- [28] Norman Mu, Alexander Kirillov, David Wagner, and Saining Xie. Slip: Self-supervision meets language-image pre-training. In *Computer Vision—ECCV 2022: 17th European Conference, Tel Aviv, Israel, October 23–27, 2022, Proceedings, Part XXVI*, pages 529–544. Springer, 2022. [2](#), [8](#)
- [29] Jaemin Na, Heechul Jung, Hyung Jin Chang, and Wonjun Hwang. Fixbi: Bridging domain spaces for unsupervised domain adaptation. In *Proceedings of the IEEE/CVF Conference on Computer Vision and Pattern Recognition*, pages 1094–1103, 2021. [2](#), [3](#)
- [30] Maria-Elena Nilsback and Andrew Zisserman. Automated flower classification over a large number of classes. In *2008 Sixth Indian Conference on Computer Vision, Graphics & Image Processing*, pages 722–729. IEEE, 2008. [7](#)
- [31] Omkar M Parkhi, Andrea Vedaldi, Andrew Zisserman, and CV Jawahar. Cats and dogs. In *2012 IEEE conference on computer vision and pattern recognition*, pages 3498–3505. IEEE, 2012. [7](#)
- [32] Alec Radford, Jong Wook Kim, Chris Hallacy, Aditya Ramesh, Gabriel Goh, Sandhini Agarwal, Girish Sastry, Amanda Askell, Pamela Mishkin, Jack Clark, et al. Learning transferable visual models from natural language supervision. In *International Conference on Machine Learning*, pages 8748–8763. PMLR, 2021. [1](#), [2](#), [3](#), [6](#), [7](#)
- [33] Kuniaki Saito, Donghyun Kim, Stan Sclaroff, Trevor Darrell, and Kate Saenko. Semi-supervised domain adaptation via minimax entropy. In *Proceedings of the IEEE/CVF international conference on computer vision*, pages 8050–8058, 2019. [2](#)
- [34] Astuti Sharma, Tarun Kalluri, and Manmohan Chandraker. Instance level affinity-based transfer for unsupervised domain adaptation. In *Proceedings of the IEEE/CVF Conference on Computer Vision and Pattern Recognition*, pages 5361–5371, 2021. [2](#), [3](#)
- [35] Khurram Soomro, Amir Roshan Zamir, and Mubarak Shah. Ucf101: A dataset of 101 human actions classes from videos in the wild. *arXiv preprint arXiv:1212.0402*, 2012. [6](#)
- [36] J. Stallkamp, M. Schlipsing, J. Salmen, and C. Igel. Man vs. computer: Benchmarking machine learning algorithms for traffic sign recognition. *Neural Networks*, (0):–, 2012. [7](#)
- [37] Yu Sun, Eric Tzeng, Trevor Darrell, and Alexei A Efros. Unsupervised domain adaptation through self-supervision. *arXiv preprint arXiv:1909.11825*, 2019. [3](#)
- [38] Yu Sun, Xiaolong Wang, Zhuang Liu, John Miller, Alexei Efros, and Moritz Hardt. Test-time training with self-supervision for generalization under distribution shifts. In *International Conference on Machine Learning*, pages 9229–9248. PMLR, 2020. [3](#)
- [39] Ashish Vaswani, Noam Shazeer, Niki Parmar, Jakob Uszkoreit, Llion Jones, Aidan N Gomez, Łukasz Kaiser, and Illia Polosukhin. Attention is all you need. *Advances in neural information processing systems*, 30, 2017. [8](#)
- [40] Bastiaan S Veeling, Jasper Linmans, Jim Winkens, Taco Cohen, and Max Welling. Rotation equivariant cnns for digital pathology. In *International Conference on Medical image computing and computer-assisted intervention*, pages 210–218. Springer, 2018. [1](#), [3](#), [7](#)
- [41] Dequan Wang, Evan Shelhamer, Shaoteng Liu, Bruno Olshausen, and Trevor Darrell. Tent: Fully test-time adaptation by entropy minimization. *arXiv preprint arXiv:2006.10726*, 2020. [2](#), [3](#), [6](#), [8](#)
- [42] Mei Wang and Weihong Deng. Deep visual domain adaptation: A survey. *Neurocomputing*, 312:135–153, 2018. [1](#)
- [43] Guoqiang Wei, Cuiling Lan, Wenjun Zeng, and Zhibo Chen. Metaalign: Coordinating domain alignment and classification for unsupervised domain adaptation. In *Proceedings of the IEEE/CVF Conference on Computer Vision and Pattern Recognition*, pages 16643–16653, 2021. [3](#)
- [44] Gui-Song Xia, Jingwen Hu, Fan Hu, Baoguang Shi, Xiang Bai, Yanfei Zhong, Liangpei Zhang, and Xiaoqiang Lu. Aid: A benchmark data set for performance evaluation of aerial scene classification. *IEEE Transactions on Geoscience and Remote Sensing*, 55(7):3965–3981, 2017. [3](#), [6](#), [7](#)
- [45] Jianxiong Xiao, James Hays, Krista A Ehinger, Aude Oliva, and Antonio Torralba. Sun database: Large-scale scene recognition from abbey to zoo. In *2010 IEEE computer society conference on computer vision and pattern recognition*, pages 3485–3492. IEEE, 2010. [7](#)
- [46] Ting Yao, Yingwei Pan, Chong-Wah Ngo, Houqiang Li, and Tao Mei. Semi-supervised domain adaptation with subspace learning for visual recognition. In *Proceedings of the IEEE conference on Computer Vision and Pattern Recognition*, pages 2142–2150, 2015. [2](#)
- [47] Lutfiah Zahara, Purnawarman Musa, Eri Prasetyo Wibowo, Irwan Karim, and Saiful Bahri Musa. The facial emotion recognition (fer-2013) dataset for prediction system of micro-expressions face using the convolutional neural network (cnn) algorithm based raspberry pi. In *2020 Fifth international conference on informatics and computing (ICIC)*, pages 1–9. IEEE, 2020. [7](#)